Biophysical Journal, Volume 98

Supporting Material

Antiport Mechanism for Cl-/H+ in ClC-ec1 from Normal Mode Analysis

Gennady V. Miloshevsky, Ahmed Hassanein, and Peter C. Jordan

Supporting Material

Antiport Mechanism for Cl^-/H^+ in ClC-ec1

from Normal Mode Analysis

Gennady V. Miloshevsky, Ahmed Hassanein and Peter C. Jordan

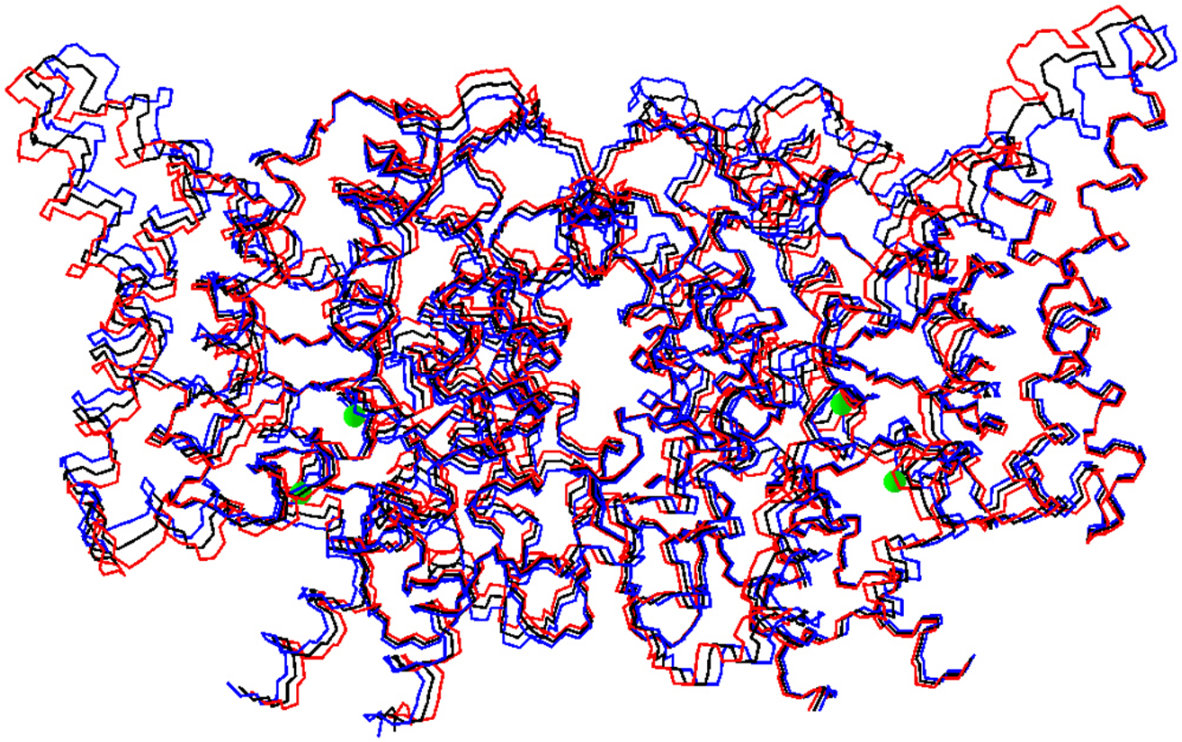

Fig. S1. Perturbation of the ClC-ec1 System along the 8th NM. Superimposed structures of ClC-ec1 in backbone representation viewed from within a membrane plane. Black backbone trace is the minimized system; red and blue traces are “positive” and “negative” displacements along the 8th NM.

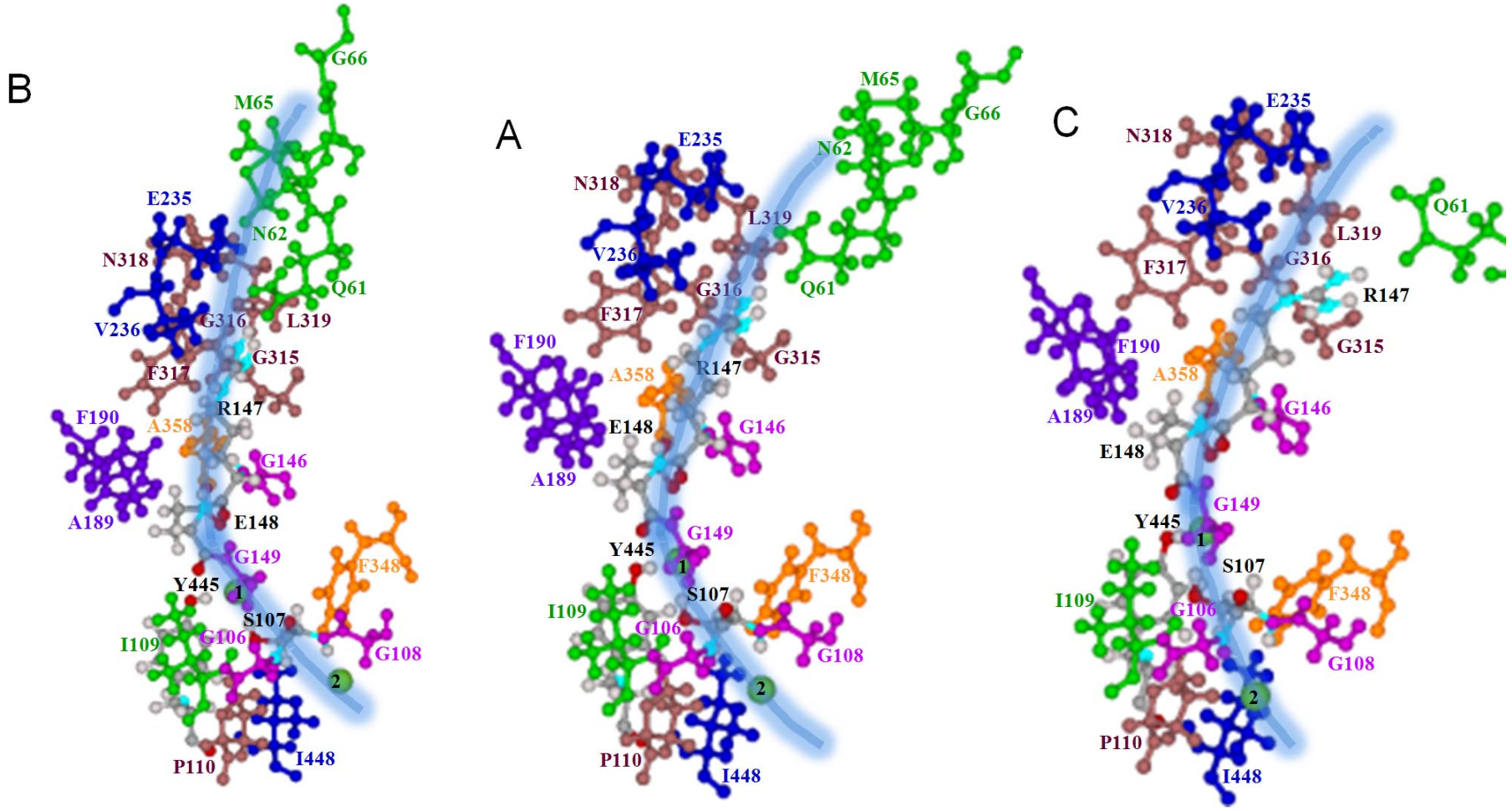

Fig. S2. The residues forming the extracellular and intracellular ClC-ec1 pores viewed from within the membrane. (**A**) Minimized ClC-ec1; (**B**) and (**C**) displacement along the 7th all-atom NM in the "positive" and "negative" directions. Only the pore of subunit A is

illustrated. The pore near the central binding site is surrounded by residues G146, R147, A358, F190 and E148, which blocks it. The side chains forming the pore near the extracellular mouth are G315, G316, F317, V236 and the guanidinium group of R147. R147 and E148 are shown in native colors. Their backbone segments are hinged to strictly conserved G146 and G149 (in pink). The others are shown in different colors: A358 – orange; A189 and F190 – violet; G315, G316, F317, N318 and L319 – brown; E235 and V236 – blue; Q61, N62, M65 and G66 - green. On the intracellular side, S107 and Y445 are shown in native colors. The backbone segment of S107 is hinged to its adjacent strictly conserved residues (G106 and G108 in pink). The others are shown in different colors: F348 – orange; I109 – green; P110 – brown; I448 – blue. Two Cl^- ions (green spheres), the one at the central binding site with label 1 and the other at the inner binding site with label 2, are shown. The pore is identified by a thick blue line. In (**A**) the E148 and S107 side chains protrude into the pore blocking the pathway on both the intracellular and extracellular sides. In (**B**) the pore is open on the intracellular side at S107 and blocked on the extracellular side. In (**C**) the intracellular pore is occluded and the extracellular pore is open assuming that E148 is protonated and dislodged. The figures are generated using our MCICP code.

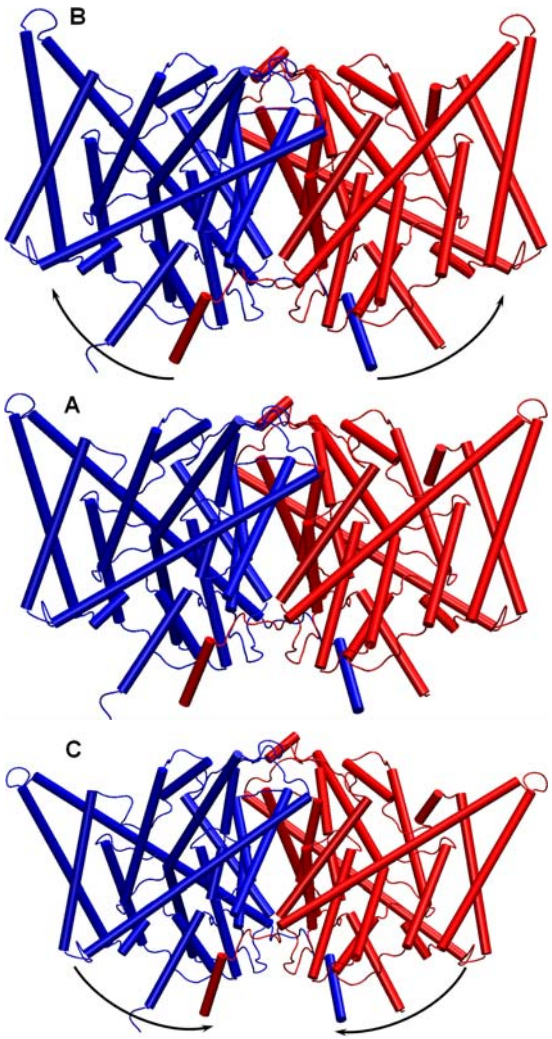

Fig. S3. Perturbation of the 207C/207C ClC-ec1 Mutant [1] along the Lowest-Frequency 7th Rotation-Translation-Block (RTB) NM. View from within a membrane plane with helices in cylinder representation. The subunit A helices are colored blue, and the subunit B ones are red. (A) The minimized system; (B) and (C), "positive" and "negative" displacement along the 7th RTB NM. The perturbation of the 207C/207C ClC-ec1 mutant in either direction along the lowest-frequency (7th) NM reveals the symmetric swinging of the subunits relative to each other. The x-ray crystal structure of the fully cross-linked 207C/207C ClC-ec1 mutant [1] at 3.1 Å resolution (PDB ID code 2R9H) was used. The 7th RTB NM was calculated using elNémo, the web-interface to the Elastic Network Model [2] freely available at http://www.igs.cnrs-mrs.fr/elnemo/index.html. This is a fast and simple tool to compute, visualize and analyze low-frequency normal modes of large biomolecules. The 2R9H file was uploaded into the elNémo web-system and the low-frequency NMs were calculated. The resulting PDB files for the requested perturbed NMs were obtained. Figures are then generated using an VMD program [3]. Animation of large-scale collective motions along the 7th RTB NM for the 207C/207C ClC-ec1 mutant directly captured from the elNémo web-page is available in **Movie S4**.

In the RTB method [4], the protein is divided into a number of rigid blocks, each consisting of one or of a few consecutive residues. In this approximation, an all-atom Hessian is projected onto a space spanned by the rotational and translational degrees of freedom of predefined protein blocks, thus effectively reducing the Hessian matrix (to a size $6n_b \times 6n_b$ with n_b a number of blocks) and the diagonalization time. The $6n_b$-length RTB NMs are then projected back to all-atom space to give a limited number, $6n_b$, of the full-length ($3N_a$) approximate all-atom NMs. The justification for using RTB NMs is that the low-frequency eigendirections are very similar in both RTB and all-atom approaches. The values of the inner products between the first few RTB and all-atom NM vectors show a high degree of overlap for conformational change among the lowest eigenvectors; however, they differ significantly for the larger eigenvectors. Thus, the low-frequency eigenvalues differ, but these quantities have no physical meaning. Only the eigendirections are meaningful. The RTB method [4] can use the detailed CHARMM22 energy function. Thus, no information is lost with respect to the electrostatic and other interactions in the RTB approximation.

Analogous ElNémo calculations were carried out on all other crystallographically resolved ClC structures. Each exhibited the same symmetric swinging of the subunits, with correlated motion of the C-termini separation and the extra- and intracellular pores. This demonstrates the qualitative equivalence of the low lying normal modes of every ClC family member crystallographically characterized.

Movies of perturbation of ClC-ec1 along the 7th NM

Movie S1. The ClC-ec1 antiporter in a cylinder representation is viewed from within plane of the membrane with the extracellular side on top. The color scheme for the helices, residues and four Cl^- ions is the same as in Figs. 1, 3, 4. Additionally, the side chains of E203 are shown in native colors. The ClC-ec1 protein undergoes large rearrangements with relative swinging of the subunits within to the membrane plane. The intracellular and extracellular permeation pathways are alternately blocked and unblocked due to the swinging motion of the CLC subunits.

Movie S2. The residues forming the extracellular pore (pore A) are viewed from within plane of the membrane. The color scheme is the same as in Fig. 3 and Fig. S2. At perturbation along the 7th NM, the R147, F317 and V236 side chains sterically block and unblock the extracellular pores of CLC-ec1. The side chains of Q61, N62 and M65 undergo large-scale motion blocking and unblocking the extracellular mouths.

Movie S3. The residues forming the intracellular pore (pore A) are viewed from the central binding site along the line toward the inner binding site. The color scheme is the same as in Fig. 4 and Fig. S2. Additionally, the side chains of E203 are shown in native colors. At perturbation along the 7th NM, the S107, Y445 and F348 side chains sterically block and unblock the intracellular pores of CLC-ec1.

Movie S4. The 207C/207C ClC-ec1mutant (PDB ID code 2R9H) [1] perturbed along the lowest-frequency RTB NM. 3D animations viewed from three orthogonal viewpoints are directly captured from the ElNémo web-page at http://www.igs.cnrs-mrs.fr/elnemo/index.html. Perturbing along the 7th RTB NM demonstrates the slow swinging motion of the ClC subunits relative to each other.

References

1. Nguitragool, W., and C. Miller. 2007. ClC Cl^-/H^+ transporters constrained by covalent cross-linking. *Proc. Natl. Acad. Sci. USA.* 104:20659-20665.
2. Suhre, K., and Y. H. Sanejouand. 2004. ElNemo: a normal mode web-server for protein movement analysis and the generation of templates for molecular replacement. *Nucleic Acids Research* 32:W610-W614.
3. Humphrey, W., A. Dalke, and K. Schulten. 1996. VMD - Visual Molecular Dynamics. *J. Molec. Graphics* 14:33-38.
4. Tama, F., F. X. Gadea, O. Marques, and Y. H. Sanejouand. 2000. Building-block approach for determining low-frequency normal modes of macromolecules. *Proteins Struct. Funct. Genet.* 41**:**1-7.